Influence of the Zn/Zr ratio in the support of a copper-based catalyst for the synthesis of methanol from CO2

Valentin l'Hospital, Laetitia Angelo, Yvan Zimmermann, Ksenia Parkhomenko, Anne-Cécile Roger

Version of Record: https://www.sciencedirect.com/science/article/pii/S0920586120302972
Manuscript_50c7e0ea964d136600c277ad2bbc5dc0

Influence of the Zn/Zr ratio in the support of a copper-based catalyst for the synthesis of methanol from CO_2

Valentin L'hospital, Laetitia Angelo, Yvan Zimmermann, Ksenia Parkhomenko, Anne-Cécile Roger

ICPEES, Research group « Energie et Carburants pour un Environnement Durable », UMR 7515 CNRS, ECPM, Université de Strasbourg, 25 Rue Becquerel, 67087 Strasbourg Cedex 2, France

ABSTRACT

CuO-ZnO-ZrO_2 catalysts were synthetized by co-precipitation synthesis. Copper content in catalysts was kept constant (30 wt% of Cu°) and ZnO was gradually substituted by ZrO_2 in the support to have a greater understanding of the support's effect and to find the optimal ZnO/ZrO_2 ratio. These catalysts were fully characterized and then tested in the methanol synthesis via CO_2 hydrogenation. The effects of reaction temperature and GHSV on the catalytic behavior were investigated. The mix of the characterization results predicted the optimum support that is composed of 50 wt% of ZnO and 50 wt% of ZrO_2 with higher metallic copper surface area and higher copper dispersion. Surprisingly the optimum catalytic results were obtained for the 30Cu-$ZZ_{66/34}$ catalyst, whose support was composed of 66 wt% of ZnO and 34 wt% of ZrO_2. This catalyst presented good CO_2 conversion (19.6%) and methanol selectivity (50%), leading to a methanol productivity of 725 $g_{MeOH}\,kg_{Cata}^{-1}\,h^{-1}$ at 280 °C, 50 bar and a GHSV of 25,000 h^{-1} (STP). Finally, the determining factor for the best catalytic activity is not the Zn/Zr ratio. To have the optimal catalytic activity in CO2 hydrogenation to methanol other parameters should be considered as well. They are: the nature and the state of copper species over the composite support; the homogeneity of the final composite sample, the ZnO particles size, and the number of ZnO-ZrO_2 interactions. The perfect combination of them all plays an important role in the determination of the best copper-based catalyst for the synthesis of methanol from CO_2.

1. Introduction

Since the mid-nineteenth century, anthropogenic Green House Gases (GHGs) emissions, especially CO_2, have risen sharply due to the industrial age and in particular to the growth in the use of fossil fuels such as coal, oil and natural gas, which are strong emitters of GHGs by combustion.

Several techniques already exist to reduce CO_2 emissions such as capture or storage. However the most promising technique is the CO_2 recovery in chemical, such as urea [1-2], salicylic acid [3], or polycarbonates [4]. Other solutions must be developed in order to further increase the proportion of anthropogenic CO_2 recovered, such as energy vectors, like methanol [5-7]. It is a very important chemical intermediate up to 80 Mt in 2016 [8]. From methanol, it is possible to produce formaldehyde [9], dimethyl ether [10-12], polymer precursors such as ethylene and propylene [13-14] as well as the MTBE [15].

Methanol is industrially synthesized from the catalytic reaction between CO and H_2 on a metal catalyst [16]. In the 1960s, a new type of catalyst was developed with copper oxide on zinc oxide, operating at temperatures of 250-350 °C and reaction pressures of 50-100 bar [17]. Then, catalysts were further optimized with alumina (Al_2O_3), this type of catalyst is still used to convert mixtures of H_2/CO/CO_2 (syngas) to methanol [18-24]. In the 1980s, kinetic and mechanistic studies only considered CO in hydrogenation, without taking CO_2 into account in the formation of methanol

[25-27]. Afterwards, complex kinetic models were developed that showed that methanol was mainly formed from CO_2 [28-30] and that this route is faster than that from CO [31]. Most copper-based catalysts for the CO_2 hydrogenation to methanol contain zinc oxide and the interaction between these two species is paramount. Metallic copper enables adsorption and dissociation of H_2 and the presence of ZnO increases the dispersion of metallic copper and thus the number of active sites in the catalyst [32-33]. It has also been shown that the addition of ZnO in a copper-based catalyst can induce the formation of such active species as Cu^+-O-Zn partially dissolved in copper particles, thereby forming a Cu-Zn alloy [34]. These sites can considerably increase the activity of the catalyst. Behrens *et al* [35] have recently shown this beneficial effect of a Cu-Zn alloy in the catalyst. The interaction between copper and zinc is therefore important, as shown in the work of Fujitani *et al* [36]. They demonstrated that it is not only metallic copper alone which is the active species in the mechanism, but also Cu-Zn sites, working together for the formation of methanol. The addition of zirconia (ZrO_2) in the support of the CuO-ZnO catalyst increases even more the dispersion of copper and zinc oxide by decreasing the crystallite size and increasing the specific surface area [37-38]. Zirconia, unlike Al_2O_3 also plays an important role in the reaction mechanism by participating in the adsorption of CO_2 due to its high basicity [32,39,40] Sintering of copper and ZnO one of the deactivation reasons could be decreased in the presence of ZrO_2 [37]. Koeppel *et al* [41] have described the Cu-ZrO_2 interface, allowing an improvement in the formation of methanol, as microcrystalline copper particles stabilized by an amorphous matrix of ZrO_2. It is therefore necessary to have a close interaction between the three species to allow the hydrogenation reaction. This synergy was confirmed recently by DFT calculation in the work of Wang *et al* [42].

Other types of catalysts as platinum-based have been studied [43], supported by various oxides, in particular supported on CeO_2 which allows to obtain very good selectivities in methanol, but low conversions of CO_2 and low durability [44]. Gold supported on ZnO has also been studied in the catalysis of CO_2 hydrogenation [45]. The Au/ZnO-TiO_2 system has similar performance to conventional catalysts of CuO-ZnO-Al_2O_3 type, but appeared to be much more expensive [46]. The use of silver as an active metal surface has also been studied [47]. Considering all others metals, the preferred one for the synthesis of methanol by the hydrogenation of CO_2 stays mainly copper [22,32,45-49] because of its abundance, low cost and high activity in the synthesis of methanol by CO_2 hydrogenation.

The most used and simplest method of catalysts' production is the co-precipitation method. The purpose of this method is to precipitate one or more metallic cations in the form of carbonates, using a precipitating agent, usually Na_2CO_3 [50-52]. The co-precipitation allows obtaining of the intimate mixture of cations at atomic level in the precipitate and thus allows a good interaction between them in the final catalyst [19], in particular between copper and zinc which have a similar atomic size. The constant and controlled pH is essential in this synthesis in order to respect the composition of the final catalyst and to favor its homogeneity.

In this study the composite CuO-ZnO-ZrO_2 materials were chosen as catalysts for CO_2 hydrogenation to methanol. In order to understand the influence of ZrO_2 presence in the support on the materials properties and their catalytic performance, the progressive substitution of ZnO by ZrO_2 in the support was performed. Several researchers have already worked on this kind of catalyst [56-59] but the optimized Zn/Zr ratio in a copper-based catalyst hasn't been studied. In our previous work the kinetic parameters of this reaction using CuO-ZnO-ZrO_2 and CuO-ZnO-Al_2O_3 catalysts were studied, showing that the activation energies are higher for alumina supported material and thus affect the selectivity to methanol [30,60]. The novelty of the present manuscript is precisely in the study of the most selective CuO-ZnO-ZrO_2 catalyst in order to understand the influence of the composition and quantity of ZrO_2 needed for the optimal composition. The materials are synthesized by conventional batch co-precipitation method with different Zn/Zr ratio keeping the same content of copper. These

catalysts were fully characterized and their catalytic performances were evaluated. The optimal chemical composition of this type of catalysts for the methanol synthesis from the CO_2 hydrogenation was presented.

2. Experimental

2.1 Preparation of catalytic materials

The CuO-ZnO-ZrO_2 (30-CuZZ) catalysts were all synthesized by the classical co-precipitation method at constant pH in batch mode [55,61]. The amount of copper was kept constant for all samples (30 wt% of Cu^0 in the final catalyst), the ZnO:ZrO_2 ratio was varied.

For the preparation of 4.00 g of fresh catalyst with ZnO:ZrO_2 mass ratio equal to 66:34, a solution of $Cu(NO_3)_2$ $3H_2O$ (19.3 mmol, 4.71 g), $Zn(NO_3)_2$ $6H_2O$ (20.4 mmol, 6.28 g) and $ZrO(NO_3)_2$ $6H_2O$ (7.1 mmol, 2.38 g) was prepared by dissolving these salts in 47 mL of distilled water, then heated to 60-65 °C, to obtain a solution with 1.0 M concentration of metallic cations (pH = -0.4). The second 1.6 M solution of Na_2CO_3 (pH = 12.4, adjusted) was prepared and used as the precipitating agent. The carbonates/nitrates molar ratio of 1.1 was chosen to have a slight excess of carbonates to ensure the complete precipitation of all the metallic cations. These solutions were added dropwise into 100 mL of water at adjusted and constant pH = 6.3 and heated at 60-65 °C. The pH and temperature were monitored during the co-precipitation step using a HI-207 HANNA pH-tester. After the reaction, the precipitate was aged with gentle stirring in the mother liquor during three hours at 60-65 °C, then filtered and washed with hot distilled water. The washing was finished when the conductivity of the filtrate was close to the distilled water, approximately 15 µS cm^{-1}, measured with a VWR CO 3100L conductimeter, meaning no ions (especially Na^+) are washed out anymore. The precipitate was then dried at 95 °C for 48 h. Afterwards the obtained solid was calcined at 400 °C for four hours with a temperature ramp of 2 °C min^{-1}. The powder obtained was sieved to reserve the particle size of 100-125 µm for catalytic tests.

The five samples with different ZnO:ZrO_2 mass ratio were prepared and abbreviated as Cu-$ZZ_{100/0}$, Cu-$ZZ_{66/34}$, Cu-$ZZ_{50/50}$, Cu-$ZZ_{34/66}$, Cu-$ZZ_{0/100}$.

2.2 Catalytic materials characterization

Specific surface area measurements were performed by nitrogen adsorption-desorption at -196 °C using the Brunauer-Emmet-Teller (BET) method on a Micromeritics ASAP 2420 apparatus. Samples were previously outgased at 250 °C overnight to remove the adsorbed moisture.

The crystalline structure of the catalysts was determined by X-ray diffraction (XRD) with a Bruker D8 Advance diffractometer equipped with a LYNXEYE detector and a Ni filter for CuKα radiations over a 2θ range between 10 and 95 ° and a step of 0.016 ° every 0.5 s. The crystallite size was calculated using the Debye-Scherrer equation. The crystallite size of CuO is calculated from the CuO (111) plane at 2θ = 38.9 ° (JCPDS 48-1548). The crystallite size of ZnO is calculated from the ZnO (100) and (110) planes at 2θ = 31.9 ° and 56.8 ° respectively (JCPDS 36-1451).

The morphology of the catalysts was studied with a ZEISS GEMINI SEM 500 scanning electron microscope with a resolution of 1.2 nm at 500 V and 1.1 nm at 1 kV, equipped with an Inlens secondary electron (SE) detector and a SE2 detector.

The elemental analysis was performed by inductively coupled plasma atomic emission spectroscopy ICP-AES. The quantitative determination of metal content in the catalysts was made based on the analysis of certificated standard solution. The sample preparation was made by dissolving 10 mg of dried and ground samples catalyst in concentrated aqua regia solution.

The X-ray photoelectron spectroscopy (XPS) measurements were performed in an ultrahigh vacuum (UHV) spectrometer equipped with a RESOLVE 120 MCD5 hemispherical electron analyzer. The Al Kα hv=1486.6 eV dual anode X-ray source was used as incident radiation. The constant pass energy mode was used to record both survey and high resolution spectra, with pass energies 100 and 20 eV respectively. The C1s peak of the adventitious carbon at 285 eV is set as reference.

Reducibility studies were performed by temperature-programmed reduction method (TPR-H_2) on a Micromeritics AutoChem II 2920 apparatus with 50 mg of fresh CuO-ZnO-ZrO_2 catalyst loading. The total gas flow rate of 10% H_2 in Ar was kept constant 50 mL min^{-1} with a heating ramp of 10 °C min^{-1} until final temperature 500 °C. The CuO reducibility was calculated in percentage from the theoretical H_2 consumption that is needed to reduce the amount of CuO in the catalyst that is determined by ICP-AES. The reaction of CuO reduction included in the calculations is following:

$$CuO + H_2 \rightarrow Cu^0 + H_2O$$

The copper metallic surface area was determined by N_2O surface reaction on a Micromeritics AutoChem II 2920 apparatus. Firstly, approximately 500 mg of fresh CuO-ZnO-ZrO_2 catalyst were reduced at 300 °C, heating rate 1°C min^{-1}, hold time 12 h, under a constant flow 50 mL min^{-1} of 10 % H_2 in Ar keeping the conditions as close to the reactional conditions as possible. Then the reduced catalyst was purged with Ar and cooled down to 50 °C. Secondly, the reduced catalyst was treated under the flow of 50 mL min^{-1} of 2 % N_2O in Ar for 15 min oxidising thus only the surficial layer of the reduced copper by N_2O to Cu_2O by following equation:

$$Cu^0 + N_2O \rightarrow Cu_2O + N_2$$

The N_2O consumption was registered with a TCD detector, according to a procedure close to those of Evans *et al*. [62] and Chinchen *et al.* [63]. The study was reported in more details in the PhD thesis of Kobl [64]. It was experimentally shown that a minimum catalyst loading is needed to get a sort of flat plateau in the TCD signal, that indicates the presence of pure N_2 in the flow, N_2O being fully consumed. This was confirmed by following simultaneously the effluent gas by both TCD and mass spectrometer (MS) for one experiment. This plateau was considered for the calculations of the N_2O consumption (see *Figure 1*).

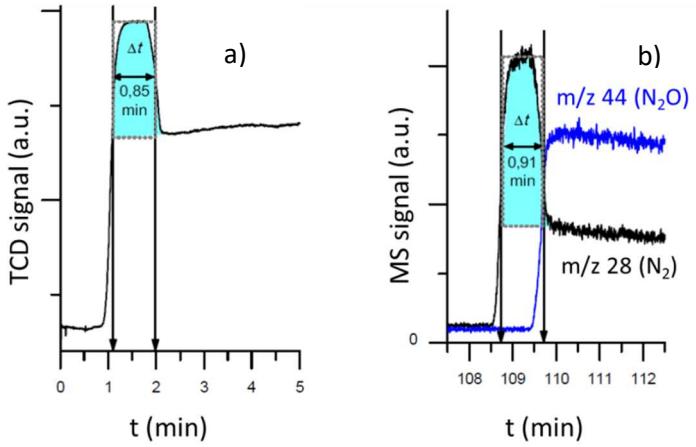

Figure 1. *Simultaneous follow-up of the reactive frontal chromatography analysis: (a) by TCD, (b) by MS. The arrows indicate the start and the end of the N_2O consumption.*

The metallic copper surface area was calculated by quantifying the amount of consumed N_2O and assumption of 1.46 10^{19} copper atoms per square meter [65]. The copper metallic dispersion was calculated according to the following formula *(2–1)*:

$$D_{Cu^\circ}(\%) = S_{Cu^\circ} \times \frac{N_S}{\omega_{Cu^\circ}} \times \frac{M_{Cu}}{N_A} \qquad (2\text{-}1)$$

With $D_{Cu^\circ}(\%)$, the metallic copper dispersion, S_{Cu°, the metallic copper surface area, N_S, the copper surface density (1.46 10^{19} atom m^{-2}), ω_{Cu°, the copper mass fraction in the catalyst, M_{Cu}, the copper molar mass and N_A, the Avogadro constant.

The TEM analyzes were made with a transmission electron microscope JEOL 2100, equipped with a LaB_6 filament and a High Resolution (HR) polar part allowing a point-to-point resolution of 0.2 nm to 200 kV (voltage) maximum equipped with an X-ray detector (EDX energy dispersive X-ray spectrometry) of the SDD (Silicon drift detector) type. The analysis was performed using a copper grid revealing a high copper content, thus only Zn and Zr content will be shown.

2.3 Catalytic activity

The catalytic tests for the methanol synthesis via CO_2 hydrogenation were carried out in a constant flow stainless-steel fixed-bed reactor. For a conventional catalytic test, the powder catalyst with 100-125 µm particle size was placed in the reactor between two beds of quartz wool held by a quartz rod, that was placed on a stainless-steel grid to prevent any movement of the catalytic bed during pressure variations. The reaction was carried out at 50 bar, between 240 and 300 °C with a gas hourly space velocity (GHSV) of 10,000 or 25,000 h^{-1} (STP).

For easier comparison of the materials' catalytic properties the total gas flow (Q_{total}) maintained constant 40.0 mL min^{-1} (STP) as well as the GHSV. The mass of different catalysts (m_{cat}) was adjusted depending on the apparent density (d_{app}) of the materials according to equation *(2-2)*. The gas molar composition is following $H_2/CO_2/N_2$ = 3.9/1.0/0.7, nitrogen is added as internal standard, hydrogen content is kept in excess in order to compare with previously reported results [55][66].

$$GHSV = \frac{Q_{total} \times d_{app}}{m_{cata}} \qquad (2\text{-}2)$$

Catalysts were reduced beforehand under a flow of H_2 of 6.2 mL min^{-1} (STP, 50 bar) with a heating ramp of 1 °C min^{-1} up to 300 °C followed by a 12 hour hold. After the reduction, the temperature was decreased to 100 °C and the reactor was then purged, still under pressure, with the reaction gases. The initial gas content was analysed and then the temperature of the reactor was increased with a heating ramp 1 °C min^{-1} up to the desired reaction temperature.

The gaseous products were analysed by online gas microchromatograph Inficon 3000, equipped with two modules: an MS5A module for the separation of H_2, N_2, CH_4 and CO, a PPQ module for separation of light gases (N_2, O_2, CO, CH_4, Ar), CO_2 and MeOH. The both modules were equipped with thermal conductivity detectors (TCD). The liquid products, water and methanol, were condensed at ambient temperature in a trap and analysed after each reaction temperature (48 h of reaction time of collection the condensate) using offline Agilent gas chromatograph 6890N, equipped with the Solgelwax column from SGE Analyticals and a flame ionization detector (FID).

The stability of the catalysts in time on stream experiments was evidenced by analyzing the gas products with online gas microchromatograph. Live monitoring of the CO formation and its ratio to the internal standard (N_2) was realized. The CO/N_2 ratio during each temperature was stable all along the catalytic test.

The conversions (CO_2 and H_2) and selectivities (MeOH and CO) were determined by the total carbon balance of the combined gas and liquid phases. The methanol productivity was calculated and expressed in two different ways: methanol productivity per catalyst mass (g_{MeOH} kg_{cat}^{-1} h^{-1}) and methanol productivity per copper surface area (mg_{MeOH} $m_{Cu^\circ}^{-2}$ h^{-1}). The calculation of TOF was done according to equation *(2-3)*.

$$TOF = \frac{Methanol\ productivity}{M_{methanol}} \times \frac{N_A}{N_S \times S_{Cu^\circ}} \qquad (2\text{-}3)$$

The thermodynamic calculations were made using the ProSimPlus3 software with a Soave-Redlich-Kwong thermodynamic model. A Gibbs reactor was used, based on the minimization of the Gibbs energy of the defined thermodynamic system (CO_2, H_2, CH_3OH, H_2O and CO).

3. Results and discussion

3.1 Characterization results

The list of the prepared catalytic materials is given in *Table 1*, where the results of all main characteristics are presented. Apparent density of the copper-based catalysts varies between 0.32 and 1.15. The increase in apparent density is linear: higher is the ZrO_2 content in the support, higher is the apparent density of the catalyst. The same phenomenon is observed for the specific surface areas. This could be explained by initially bigger specific surface area of the pure zirconium oxide comparing to pure ZnO, 46 vs 16 $m^2\ g^{-1}$ respectively (*Table 1*). The smallest surface area, 41 $m^2\ g^{-1}$, was observed for 30Cu-$ZZ_{100/0}$ and the highest surface area, 156 $m^2\ g^{-1}$, is determined for 30Cu-$ZZ_{0/100}$. The same observations were reported by Liu *et al* [67]. With the increased ZrO_2 content in the catalyst support, the pore morphology is modified. *Fig. 2* displays the nitrogen adsorption-desorption isotherms and the pore size distribution. All isotherms (*Fig. 2a*) are of type IV with a small hysteresis loop which is increased with increasing ZrO_2 content in the support, indicating the progressive formation of mesopores in Zr-containing samples. Without zirconia, the 30Cu-$ZZ_{100/0}$ catalyst's isotherms are quite flat indicating that it obviously does not possess high porosity. Having only zirconia in the support the hysteresis loop on the isotherms is more visible and some mesopores (4 nm) appear as shown on the pore size distribution graph (*Fig.2b*).

Fig. 3 shows the X-ray diffractograms of calcined materials. Zirconia is supposed to be in an amorphous or nanocristallite state and was not observable. The size of CuO crystallites is between 9 and 13 nm and without obvious dependence on the ZnO/ZrO_2 ratio for ZnO-containing samples.

Table 1. *Characterization results of the fresh 30Cu-ZnZr catalysts*

Catalyst	d_{app}[a] ($g\ cm^{-3}$)	BET S_{BET}[b] ($m^2\ g^{-1}$)	D (nm)[c] CuO	D (nm)[c] ZnO	CuO reducibility (%)[d]	S_{Cu°[e] ($m^2_{Cu^\circ}\ g_{cata}^{-1}$)	D_{Cu°(%)	Content (wt%)[f] Cu	Content (wt%)[f] Na
30Cu-$ZZ_{100/0}$	0.32	41	12	13	91.2	6.4	3.3	31	0.01
30Cu-$ZZ_{66/34}$	0.51	79	10	10	95.1	10.5	5.4	30	-*
30Cu-$ZZ_{50/50}$	0.84	97	12	9	94.3	12.4	6.4	30	0.07
30Cu-$ZZ_{34/66}$	0.97	109	13	11	93.4	11.1	5.7	30	0.09
30Cu-$ZZ_{0/100}$	1.15	156	11	-	96.1	4.4	2.3	29	0.11
CuO		16							
ZnO		29							
ZrO_2		46							

[a] Apparent density
[b] Specific surface area
[c] Crystallite size determined by XRD using the Debye-Scherrer equation
[d] CuO reducibility calculate from the amount of consumed H_2
[e] Copper metallic surface area obtained by N_2O surface reaction
[f] Content of each element determined by ICP-AES, the oxygen content wt% is not presented
* could not be determined due to technical limitations – very small quantity

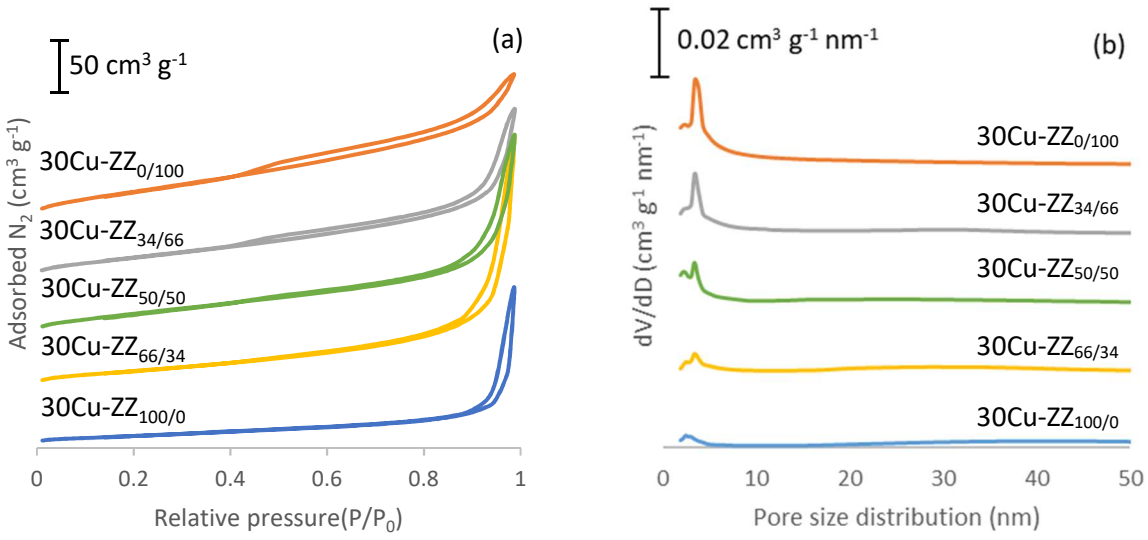

Figure 2. *(a) Adsorption/desorption isotherms and (b) pore size distribution of 30Cu-ZZ fresh catalysts*

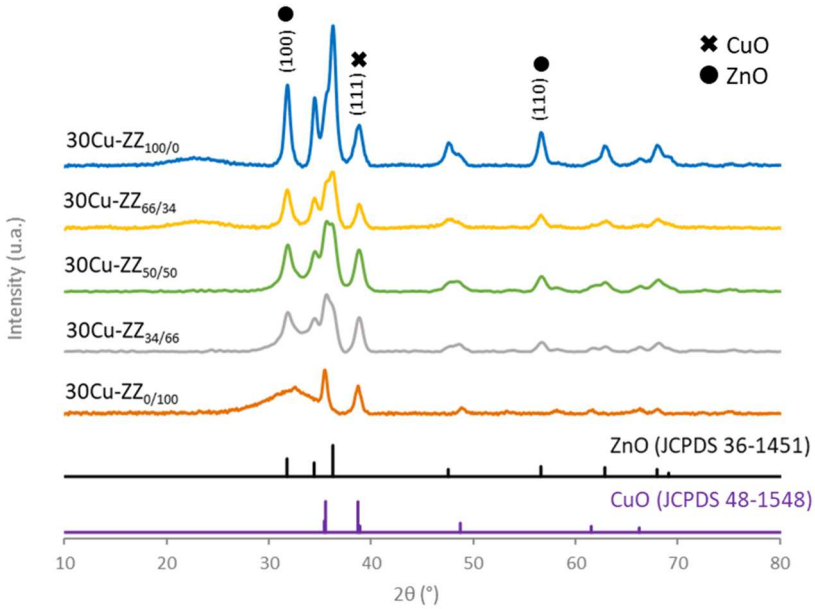

Figure 3. *X-ray diffractograms of 30Cu-ZZ fresh catalysts.*

Prior to the analysis of composite catalysts, the H_2-TPR experiments were carried out in the same conditions for the single oxides ZnO and ZrO_2. No reduction was observed in both cases. H_2-TPR profiles of the Cu-containing materials are shown in *Figure 4*. The reduction of the copper oxide for the catalyst free of zirconia 30Cu-$ZZ_{100/0}$ occurs around 235 °C, in the form of a single large peak with little foregoing and behind shoulders with total H_2 consumption equal to 4.17 $mmol_{H2}$ g^{-1}. The peak is more defined than those of other reduction profiles and indicates a more homogeneous size distribution of reducible copper oxide species. When the ZrO_2 content is increased to 34 % in the catalyst support, the reduction temperature of CuO decreases and the H_2 consumption increases (4.49 $mmol_{H2}$ g^{-1} for 30Cu-$ZZ_{66/34}$). The behind shoulder peak becomes visible, indicating some heterogeneity in the copper oxide species formed. In this case it is likely that there are two possible types of interaction of CuO with the ZnO/ZrO_2 support: CuO may interact with ZnO and with ZrO_2 separately. The further increase of Zr content in the samples brings the enlargement of the reduction

peaks and more visible separation of the foregoing shoulder, the behind shoulder is observable only for the 30Cu-$ZZ_{66/34}$ sample. As the ZrO_2 content increases from 34 to 50 %, a peak shoulder is progressively transformed into a second reduction zone when the ZrO_2 content increases from 50 to 66 % in the support until splitting completely with a content of 100 % ZrO_2 in the support. The highest H_2 consumption is reached at 100 % ZrO_2 in the catalyst support: 4.69 $mmol_{H2}$ g^{-1} for 30Cu-$ZZ_{0/100}$ and indicates the highest reducibility among all the samples (*Table 1*). The decrease in the CuO reduction temperature and the increase in H_2 consumption, when the ZrO_2 amount increases, probably indicates smaller particle size of CuO and thus weaker interaction between CuO species and the support [67][68]. This fact confirms that the presence of Zn is still necessary for the interaction and stabilization of CuO with the support. The H_2 consumption was used for the calculation of the reducibility of CuO species in the catalysts, the chemical composition of the catalysts was determined beforehand (*Table 1*). In the sample 30Cu-$ZZ_{100/0}$ with only ZnO present in the support the reducibility is the smallest indicating quite strong interactions between CuO and ZnO. The presence of ZrO_2 increases slightly the reducibility and thus accessibility of copper species for catalysis. When there is no ZnO, but only ZrO_2 present in the support, the reduction is clearly carried out in two stages: the first zone of consumption of H_2 before 200 °C and the second around 220 °C. This splitting can be explained by different insertions or interactions between the copper and the support [69] or by a heterogeneous distribution of CuO particles by their size [70].

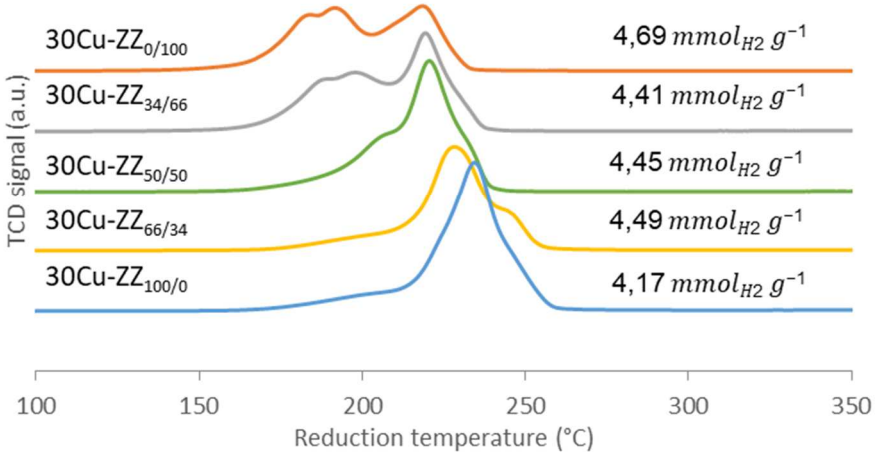

Figure 4. *H_2 consumption during TPR for 30Cu-ZZ fresh catalysts.*

Additional XPS studies were performed for some samples in order to observe the elemental composition over the surface and combine the results with H_2-TPR experiments. *Figure 5* displays the total survey scan for the 30Cu-$ZZ_{34/66}$ sample as well as the high resolution spectrum for Cu2p region. The XPS peaks of all elements that exist in the samples surface are detected in the survey scans. High resolution XPS spectra of all elements were also acquired. The shape and position of the Zn2p, Cu2p and Zr3d peaks are characteristic of previously reported data on ZnO, ZrO_2 and CuO respectively [68]. The shape of the high resolution spectrum for Cu2p region was the same for all tested samples indicating the presence of only Cu^{2+} species (*Fig. 5b*). Two possible copper species could be present over the materials surface: CuO and $Cu(OH)_2$ [71].The presence of hydroxyl species is very likely due to the moderate calcination temperature of the materials and due to the formation of malachite-like hydroxo-carbonates during the co-precipitation synthesis. The presence of these species could confirm the heterogeneous reduction profiles obtained during the H_2-TPR experiments where different types of copper-support interactions were observed. The surface composition of all elements was calculated by using the area of the core level peaks, normalized to the photoemission cross section by assuming a homogeneous distribution arrangement model. The surface atomic ratios of all elements of all tested samples are summarized in *Table 2*. It was evidenced once again that the presence of Zr in the

materials support make the copper more accessible and present on the surface – the weight content of copper is similar in all samples (*Table 1*) but the atomic content on the surface (*Table 2*) is much smaller for the 30Cu-$ZZ_{0/100}$ sample, without Zn. The traces of sodium that were found in the samples (*Table 1*) were not considered as significant and thus their presence was not discussed in terms of affection the characterization and catalytic results.

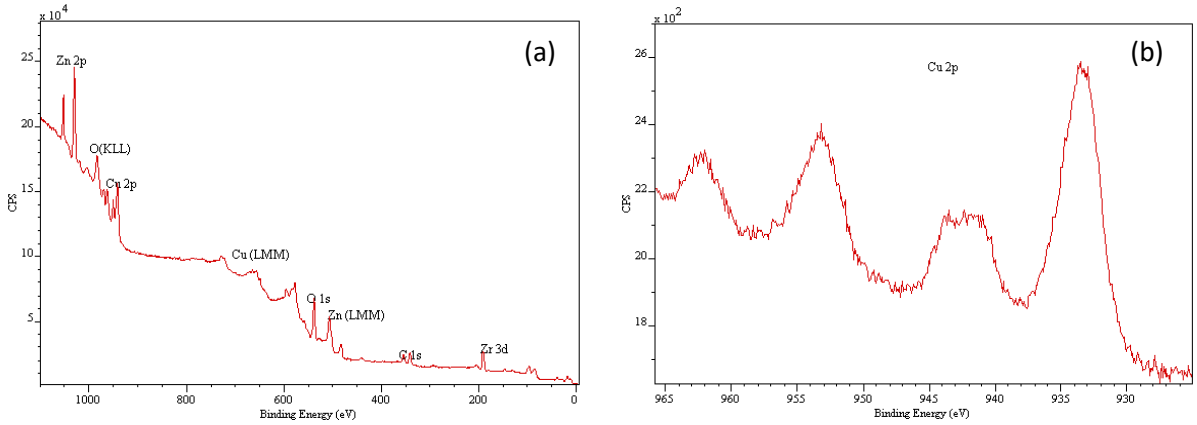

Figure 5. *XPS spectra of the 30Cu-$ZZ_{34/66}$ sample: survey scan spectrum (a) and high resolution spectrum for Cu2p (b).*

Table 2. *Surface atomic composition of the fresh 30Cu-ZnZr catalysts*

Catalyst	Content (%)[a]			
	Cu	Zn	Zr	O
30Cu-$ZZ_{100/0}$	13.3	32.4	0	54.3
30Cu-$ZZ_{66/34}$	-[b]	-	-	-
30Cu-$ZZ_{50/50}$	15.4	22.5	5.8	56.4
30Cu-$ZZ_{34/66}$	17.6	14.6	9.8	58.0
30Cu-$ZZ_{0/100}$	17.8	0	17.7	64.5

[a] determined by XPS analysis

[b] could not be determined due to technical limitations

Figure 6 illustrates the variation of the copper metallic surface area as a function of the mass content of ZrO_2 in the support. Here the copper defects that could be present according to the work of Fichtl *et al* [72] were not considered. All the copper surface area measurements of the present catalytic materials family, that were prepared by the same synthesis method, were performed in the same conditions. The results are shown on the *Fig.6*. When the catalyst support is composed only of ZnO or ZrO_2 oxide, the copper metallic surface area is the lowest (6.4 and 4.4 $m_{Cu^0}^2\ g_{Cata}^{-1}$ for 30Cu-$ZZ_{100/0}$ and for 30Cu-$ZZ_{0/100}$, respectively) despite their great difference in specific surface area measured by BET method and quite high atomic copper presence on the surface for 30Cu-$ZZ_{0/100}$ sample. This shows that the metallic copper surface area is not necessarily related to the specific surface area of the material but depends on the interactions between metallic Cu and the support. Indeed, when the two oxides (ZrO_2 and ZnO) are simultaneously present in the support, the metallic copper is more efficiently dispersed and reaches the highest metallic copper surface area 12.4 $m_{Cu^0}^2\ g_{Cata}^{-1}$ for the mass ZnO/ZrO_2 ratio of 50/50. The simultaneous presence of ZnO and ZrO_2 in the support allows the increase of the metallic copper surface area of the catalyst. The metallic copper dispersion follows the same trend; the results are displayed in *Table 1*. The lowest dispersion when the support is composed of only one oxide (3.3 % and 2.3 %, for 30Cu-$ZZ_{100/0}$ and 30Cu-$ZZ_{0/100}$, respectively). When the support of the catalyst is composed of the same amount of Zn and Zr (by mass of oxides) the metallic copper dispersion is the highest, 6.4 % for 30Cu-$ZZ_{50/50}$.

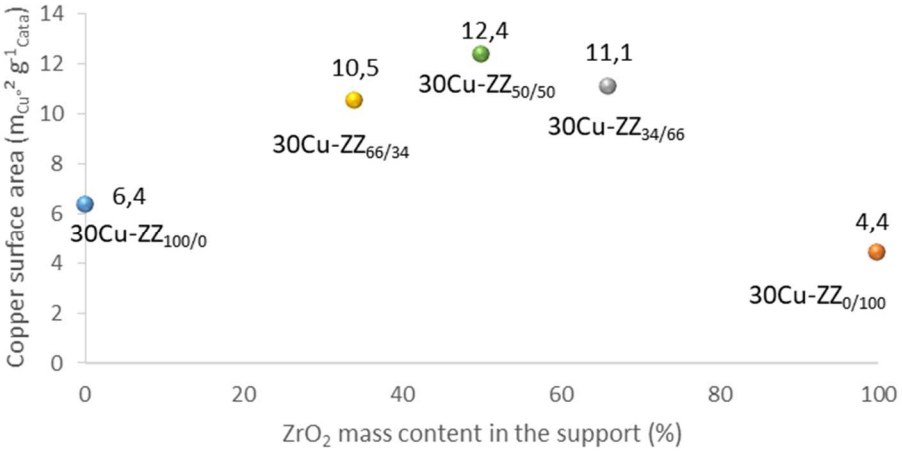

***Figure 6**. Metallic copper surface area as a function of the ZrO_2 mass content in the support.*

The 30Cu-$ZZ_{66/34}$ catalyst only was analyzed by TEM, the images are shown in *Figure 7*. Two distinct types of crystals of different sizes were observed. Zone A (*Fig. 7a*) is composed of large crystals, in the range of 20-30 nm, which is larger than the size of the crystallites determined by XRD (*Table 1).* Zone B (*Fig. 7a*) seems rather granular with small crystals (about 4 to 7 nm). The heterogeneity of the crystal sizes was confirmed by visualizing different particles (*Fig. 7b* and *7c*). A zone of fine grains, similar to an amorphous phase on the edge of the crystals, is observed (orange arrows, *Fig. 7b* and *7c*). This amorphous phase could be attributed to ZrO_2 thus, explaining the absence of characteristic lines in XRD.

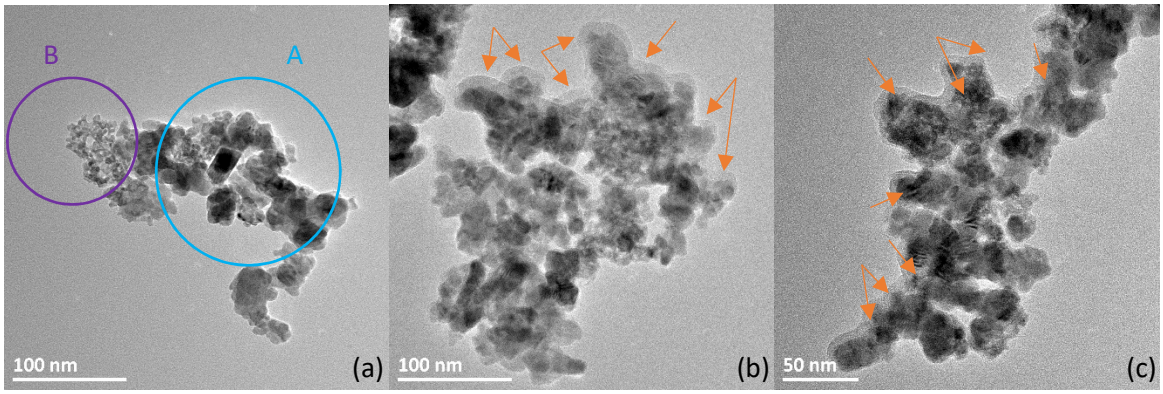

***Figure 7**. TEM images in light field for the 30Cu-$ZZ_{66/34}$ fresh catalyst.*

Energy dispersive X-ray spectroscopy (EDX) was used to analyse the composition of different zones. The results are presented in *Figure 8*. They have to be compared with the theoretical mass contents of the individual oxides in the catalyst: 41.5 wt% of ZnO and 21.0 wt% of ZrO_2 for 30Cu-$ZZ_{66/34}$. Zone C (*Fig. 8a* and *8b*), similar to zone A of *Fig. 7a*, appears rather dark and compact and contains 42 wt% of ZnO and only 3 wt% of ZrO_2. Zone D (*Fig. 8a* and *8c*), rather granular, similar to zone B of *Fig.7a*, contains 25 wt% of ZnO and 35 wt% of ZrO_2. The zone D, composed of small crystals is a great deal richer in ZrO_2 than the zone C, poor in ZrO_2, composed of larger crystals. The values of the mass compositions obtained for zone C are very far from the theoretical composition, unlike zone D which approaches it, but which still contains more zirconium and less zinc. These results could explain the splitting of the H_2-TPR profile in to peaks. It is suggested that smaller particles are reduced at lower temperature and the bigger particles having higher content of Zr and thus stronger copper-support interaction are reduced at higher temperature. The EDX analysis clearly

showed the heterogeneity of chemical composition in the bulk of the material and confirmed the presence of different interactions between copper and the support conditioned by this heterogeneity.

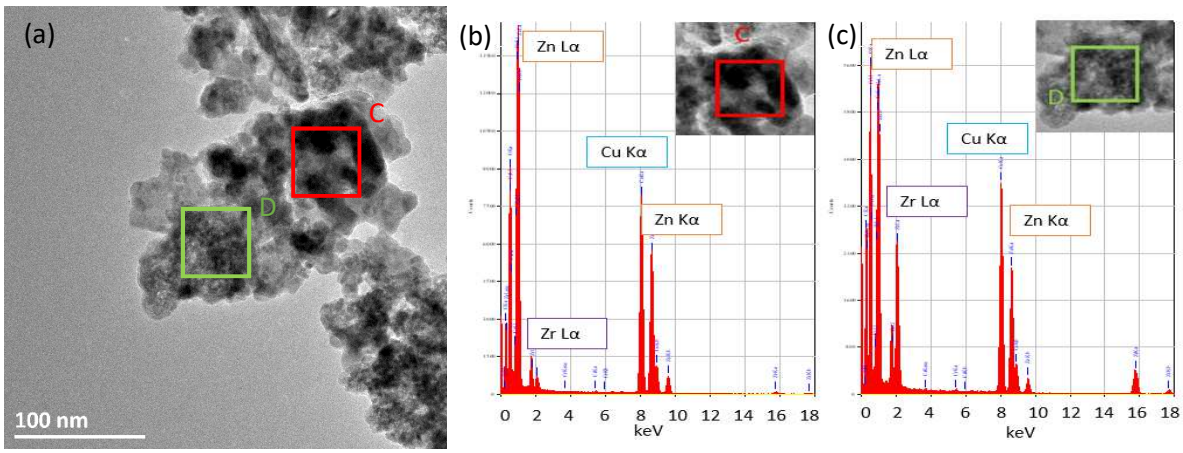

***Figure 8**. Light field TEM image of 30Cu-ZZ$_{66/34}$ fresh catalyst (a) and EDX analysis of zone C (b) and zone D (c).*

According to the physicochemical characterizations carried out for batch co-precipitated CZZ catalysts, the most promising catalysts are the materials composed of all three oxides (CuO, ZnO and ZrO_2). They have the best metallic copper surface areas as well as a strong interaction between copper and the support.

3.2 CO_2 hydrogenation to methanol

The 30Cu-ZZ catalysts were tested in the methanol synthesis by CO_2 hydrogenation. The catalytic results obtained for the five prepared catalysts with different ZnO/ZrO_2 ratios are shown in *Table 3*. The catalyst mass is not the same and was adapted for each test in order to keep the same GHSV for easier comparison. The catalysts loading is conditioned by their apparent density which increases with increasing the Zr content (*Table 1*).

***Table 3**. Catalytic Results at 50 bar and 10 000 h^{-1}.*

Catalyst	Catalyst mass (mg)	T (°C)	Conversion (%)		Selectivity (%)		MeOH yield (%)	MeOH productivity		TOF (10^{-3} s^{-1})
			CO_2	H_2	MeOH	CO		By catalyst mass (g_{MeOH} kg_{cat}^{-1} h^{-1})	By Cu° surface (g_{MeOH} $m_{Cu°}^{-2}$ h^{-1})	
30Cu-ZZ$_{100/0}$	76.8	240	9.1	4.3	42	58	3.8	281	43.9	15.7
		260	15.4	6.8	33	67	5.1	378	59.1	21.1
		280	21.2	8.7	28	72	5.9	435	68.0	24.3
		300	24.6	9.1	21	79	5.2	380	59.4	21.3
30Cu-ZZ$_{66/34}$	122.4	240	13.7	7.2	50	50	6.9	314	29.9	10.7
		260	19.6	9.4	50	50	9.8	453	43.1	15.4
		280	22.2	10.0	34	66	7.5	346	33.0	11.8
		300	24.0	9.6	22	78	5.3	248	23.6	8.5
30Cu-ZZ$_{50/50}$	201.6	240	/	/	/	/	/	/		/
		260	17.2	7.5	39	61	6.7	189	15.3	5.5
		280	21.9	10.1	37	63	8.1	230	18.5	6.6
		300	24.0	9.8	28	72	6.6	188	15.2	5.4
30Cu-ZZ$_{34/66}$	232.8	240	14.3	7.3	45	55	6.5	159	14.3	5.1
		260	23.6	11.0	45	55	10.7	261	23.6	8.4
		280	25.4	10.9	36	64	9.1	223	20.1	7.2
		300	/	/	/	/	/	/	/	/

30Cu-ZZ$_{0/100}$	276.0	240	13.2	7.0	53	47	7.0	145	33.0	11.8
		260	18.6	9.0	43	57	8.0	167	38.0	13,6
		280	23.2	9.6	29	71	6.7	139	31.6	11.3
		300	25.7	10.1	22	78	5.7	115	26.1	9.4
Thermo	/	240	33.4	22.4	80	20	26.8	/	/	/
		260	30.5	17.8	64	36	19.4	/	/	/
		280	29.5	14.3	44	56	13.0	/	/	/
		300	30.1	11.9	27	73	8.1	/	/	/
State of the art										
30CuZn–Z [55]	/	280	23.2	9.8	33	67	/	331	26.0	9.3
CuZnZr [73]	/	240	22.4	/	64	/	/	620	8.5	3.0
CZAZ-0Al [48]	/	250	25.9	/	62	/	/	219	7.3	2.6
M-CZZ(16) [42]	/	220	18.2	/	80	/	/	297	/	20
C6Z3Z1-OX [39]	/	240	18.0	/	51	/	/	305	10.9	3.9

For all the catalysts, the CO_2 and H_2 conversions increase with the reaction temperature and tend towards the thermodynamic values. During the CO_2 hydrogenation in these conditions apart from the methanol synthesis (*eq. 1*) the reverse water gas shift reaction (RGWS) (*eq. 2*) takes place in the same time. As the temperature increases, the methanol selectivity decreases. The CO selectivity increases simultaneously and CO becomes predominant in the reaction products due to the kinetics of RWGS which are faster at high temperatures than for the methanol synthesis reaction.

$$CO_2 + 3H_2 \leftrightarrows CH_3OH + H_2O \qquad \Delta_rH^\circ_{25°C} = -49.8 \text{ kJ.mol}^{-1} \qquad \textit{eq. (1)}$$

$$CO_2 + H_2 \leftrightarrows CO + H_2O \qquad \Delta_rH^\circ_{25°C} = 41.0 \text{ kJ.mol}^{-1} \qquad \textit{eq. (2)}$$

When the temperature increases, the catalyst 30Cu-$ZZ_{100/0}$ presents the lowest CO_2 conversion (9.4 % at 240 °C). The addition of ZrO_2 in the support allows increasing the conversion to approximately 14 % for the catalysts 30Cu-$ZZ_{66/34}$ and 30Cu-$ZZ_{34/66}$ at the same temperature. Catalysts 30Cu-$ZZ_{66/34}$ and 30Cu-$ZZ_{34/66}$ also show the most appropriate conversions of H_2 at 240 °C with 7.2 and 7.3 %, respectively. The conversions of H_2 and CO_2 increase with temperature and approach thermodynamic values at high temperature (300 °C): approximately 25 % for CO_2 and 10 % for H_2 (*Table 3*).

MeOH selectivity drops rapidly from 240 to 300 °C in all cases, to the benefit of the formation of CO. However, the increase of ZrO_2 content in the support plays a positive role for MeOH selectivity: growth from 33 % for 30Cu-$ZZ_{100/0}$ (at 260 °C) to 50 % for the catalysts 30Cu-$ZZ_{66/34}$ (at 240 °C) at the same CO_2 conversion (14-15 %). By comparing methanol selectivities at the same CO_2 conversion for all the catalysts, the 30Cu-$ZZ_{66/34}$ catalyst leads to the highest methanol selectivity: 50 % at 14 % CO_2 conversion (240 °C).

When ZnO is progressively substituted by ZrO_2 in the catalyst support, methanol yield can reach the maximum of 10.7 % for the catalyst 30Cu-$CZZ_{34/66}$ at 260 °C. However, when all ZnO is substituted with ZrO_2, the methanol yield decreases for the catalyst 30Cu$ZZ_{0/100}$. This indicates that the presence of both oxides in the catalyst support, ZnO and ZrO_2, is necessary to improve catalytic performance, the matter is to find their optimal content.

From the characterization results it could be supposed that the best catalytic activity would be expected for the 30Cu-$CZZ_{50/50}$ sample with biggest metallic copper surface area and copper dispersion. It appears that this catalyst does not systematically show the most optimal catalytic performance. This observation agrees with the work of Wang *et al* [42]. When catalytic performance is evaluated as MeOH productivity per mass of catalyst (*Fig. 9a*), the effect of the progressive substitution of ZnO by ZrO_2 is significant. Indeed, when ZrO_2 content increases in the catalyst support, MeOH productivity decreases rapidly. An exception is observed for the catalyst 30Cu-$ZZ_{66/34}$. Thus, this catalyst has the greatest productivity, 453 $g_{MeOH}\, kg_{cat}^{-1}\, h^{-1}$ at 260 °C. When the ZrO_2 content exceeds 34 wt% in the support, the productivity of methanol per catalyst mass decreases: 167 $g_{MeOH}\, kg_{cat}^{-1}\, h^{-1}$at 260 °C for 30Cu-$ZZ_{0/100}$. Our catalysts are still competitive compared to the other catalysts

in the literature (*Table 3*), even if it is always difficult to compare the catalytic results because of the different catalytic test conditions and some missing information in the papers.

By plotting the methanol productivity as a function of the metallic copper surface area (*Fig. 9b*), no relationship of proportionality between these two quantities appears. This is consistent with the fact that TOF numbers, based only on Cu° as active sites, vary from one Cu-ZZ catalyst to another (see *Table 3*). It is suggested that the determining factor for the catalytic activity is more complicated than simply the nature and the state of copper species. Other parameters that could play a role are the ZnO particle size or the number of oxygen vacancies generated by the ZnO-ZrO_2 interactions [42].

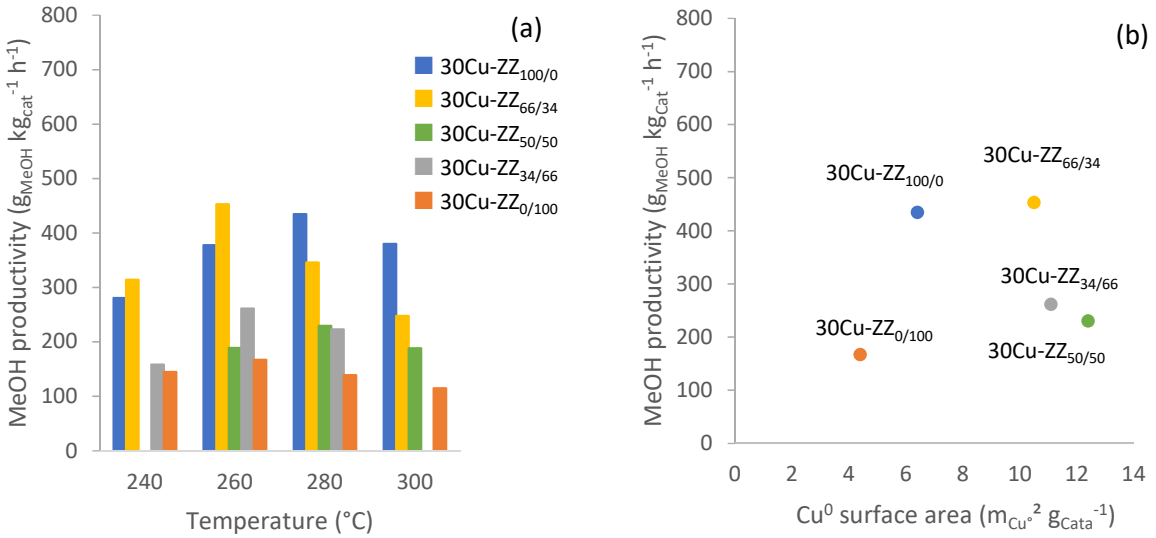

***Figure 9**. CH_3OH productivity per catalyst mass at different temperatures under 50 bar and a GHSV (STP) of 10,000 h^{-1} (a) and CH_3OH productivity per metallic copper surface at different temperatures under 50 bar and a GHSV (STP) of 10,000 h^{-1} (b).*

3.3 Effect of GHSV

The influence of GHSV on methanol productivity was studied by varying the catalyst mass under the same flow of reactants. The results obtained with the 30Cu-$ZZ_{66/34}$ catalyst at GHSV 10,000 h^{-1} and 25,000 h^{-1} are presented in *Table 4*. CO_2 conversion decreases from 22.2 % to 17.9 % and the H_2 conversion decreases from 10.0 % to 7.4 % at the reaction temperature 280 °C, when GHSV increased from 10,000 to 25,000 h^{-1}. At the same reaction temperature, methanol selectivity is almost not affected by gas velocity, 34 % and 36 % for 10,000 h^{-1} and 25,000 h^{-1}, respectively.

According to the work of Arena *et al* [73] when the GHSV increases, the specific CO_2 reaction rate (mol_{CO2} g_{cat}^{-1} s^{-1}) increases linearly. Here the methanol productivity is increased from 346 to 725 g_{MeOH} kg_{Cata}^{-1} h^{-1} when GHSV is increased from 10,000 to 25,000 h^{-1} (STP). The same observation is made for the other reaction temperatures as shown in *Table 4* confirming the absence of diffusional limitations and getting the possibility of higher methanol production per masse of catalyst and per unit of time.

***Table 4**. Catalytic results at different GHSV and 50 bar for the 30Cu-$ZZ_{66/34}$ catalyst.*

Catalyst 30Cu-$ZZ_{66/34}$	**Catalyst mass (mg)**	**T (°C)**	**Conversion (%)**		**Selectivity (%)**		**MeOH yield (%)**	**MeOH productivity (g kg_{cata}^{-1} h^{-1})**	**TOF (10^{-3} s^{-1})**
			CO_2	**H_2**	**MeOH**	**CO**			
10,000 h^{-1}	122.4	240	13.7	7.2	50	50	6.9	314	10.7

		260	19.6	9.4	50	50	9.8	453	15.4
		280	22.2	10.0	34	66	7.5	346	11.8
		300	24.0	9.6	22	78	5.3	248	8.5
25,000 h^{-1}	48.0	240	6.9	2.6	48	52	3.3	378	12.9
		260	12.5	5.6	45	55	5.7	641	21.8
		280	17.9	7.4	36	64	6.4	725	24.7
		300	22.7	8.6	27	73	6.1	692	23.6

4. Conclusions

The progressive substitution of ZnO by ZrO_2 in the support of copper-based materials has shown the effect of the presence of ZrO_2 on the physicochemical characteristics and on the catalytic performances for the methanol synthesis from CO_2.

With this progressive substitution, the apparent density of the catalysts, as well as the specific surface area and the reduction temperature of CuO increase with ZrO_2 content. Different CuO-support interactions were formed when ZrO_2 was introduced. Copper surface area is the lowest for catalyst supports composed of a single oxide (6.4 and 4.4 $m_{Cu^0}^2$ g^{-1} for 30Cu-$ZZ_{0/100}$ et 30Cu-$ZZ_{100/0}$, respectively) but increases strongly with the combined presence of ZnO and ZrO_2 in the support (up to 12.4 $m_{Cu^0}^2$ g^{-1} for 30Cu$ZZ_{50/50}$. Pure zirconia as the catalyst support has no interest in terms of the dispersion of metallic copper. The interactions between ZnO and ZrO_2 help to increase both the copper dispersion and metallic surface area.

The catalysts were tested at 10,000 h^{-1} (STP) at the CO_2 hydrogenation to methanol. The catalyst 30Cu-$ZZ_{66/34}$ showed a maximal methanol productivity by catalyst mass (453 g_{MeOH} kg_{cat}^{-1} h^{-1} at 260 °C with a methanol selectivity of 50% and a CO_2 conversion of 19.6%). However, increase of ZrO_2 content in the catalyst support decreases methanol production. By increasing GHSV to 25,000 h^{-1} (STP), CO_2 and H_2 conversions decrease, MeOH selectivity increases, resulting in a higher methanol productivity of 725 g_{MeOH} kg_{Cata}^{-1} h^{-1} at 280 °C and bringing the prepared material on the high level of methanol productivity known in the state-of-the-art. It was proven that the combined presence of both ZnO and ZrO_2 within the copper catalyst support is necessary. Finally, the determining factor for the best catalytic activity is not the Zn/Zr ratio. It is more complicated than a simple nature and the state of copper species over the composite support. Other parameters as the homogeneity of the final composite sample, the ZnO particles size, and the number of ZnO-ZrO_2 interactions could play an important role in the determination of the best copper-based catalyst for the synthesis of methanol from CO_2.

Acknowledgements

The authors are grateful to Thierry Romero (ICPEES, Strasbourg) and Corinne Bouillet (IPCMS, Strasbourg) for the TEM analyses, and to Vasiliki Papaefthymiou (ICPEES, Strasbourg) for the XPS analysis. The authors acknowledge the ANR for financial support (project DIGAS N°ANR-14-CE05-0012). The authors thank Daniel Schwarz (University of Strasbourg) for correcting the English language.

References

[1] F. Shi, Y. Deng, T. SiMa, J. Peng, Y. Gu, and B. Qiao, "Alternatives to phosgene and carbon monoxide: Synthesis of symmetric urea derivatives with carbon dioxide in ionic liquids," Angew. Chemie - Int. Ed. 42, (28), 2003, 3257–3260.

[2] E. Koohestanian, J. Sadeghi, D. Mohebbi-Kalhori, F. Shahraki, and A. Samimi, “A novel process for CO_2 capture from the flue gases to produce urea and ammonia,” Energy. 144, 2018, 279–285.

[3] M. Aresta, A. Dibenedetto, and A. Angelini, Converting “Exhaust” Carbon into “Working” Carbon, 1st ed., 66. Elsevier Inc., 2014.

[4] M. Taherimehr and P. P. Pescarmona, “Green polycarbonates prepared by the copolymerization of CO_2 with epoxides,” J. Appl. Polym. Sci., 131, (21), 2014, 1–17.

[5] A. Goeppert, M. Czaun, J. Jones, G. K. S. Prakash, and G. A. Olah, “Recycling of carbon dioxide to methanol and derived products – closing the loop,” Chem. Soc. Rev. (23), 2014.

[6] G. a Olah, A. Goeppert, and G. K. S. Prakash, “Chemical recycling of carbon dioxide to methanol and dimethyl ether: from greenhouse gas to renewable, environmentally carbon neutral fuels and synthetic hydrocarbons.,” J. Org. Chem. 74, (2), 2009, 487–498.

[7] G. A. Olah, G. K. S. Prakash, and A. Goeppert, “Anthropogenic Chemical Carbon Cycle for a Sustainable Future,” J. Am. Chem. Soc. 123 , 2011, 12881–12898.

[8] M. Alvarado, “IHS CHEMICAL Slower growth but strong prospects Uncertainty heightening structural change,” 3, 2016, 10–11.

[9] O. S. Santos, A. J. S. Mascarenhas, and H. M. C. Andrade, “Short communication N_2O-assisted methanol selective oxidation to formaldehyde on cobalt oxide catalysts derived from layered double hydroxides,” Catal. Commun., 113, 2018, 32–35.

[10] M. Xu, “A : Synthesis of dimethyl ether (DME) from methanol over solid-acid catalysts,” Appl. Catal. A: Gen. 149, 1997, 289–301.

[11] W. Pranee, S. Neramittagapong, P. Assawasaengrat, and A. Neramittagapong, “Dimethyl ether synthesis from methanol over diatomite catalyst modified using nitric acid treatment,” Energy Sources, Part A Recover. Util. Environ. Eff. 38, (15), 2016, 2244–2249.

[12] F. Xiong et al., “Methanol Conversion into Dimethyl Ether on the Anatase TiO_2(001) Surface,” Angew. Chemie - Int. Ed. 55, (2), 2016, 623–628.

[13] F. J. Keil, “Methanol-to-hydrocarbons : process technology,” Microporous Mesoporous Mater. 29, 1999, 49–66.

[14] M. Aresta, A. Dibenedetto, and A. Angelini, “The changing paradigm in CO_2 utilization,” J. CO_2 Util. 3–4, 2013, 65–73.

[15] C. P. Nicolaides, C. J. Stotijn, E. R. A. Van Der Veen, and M. S. Visser, “Conversion of methanol and isobutanol to MTBE,” Appl. Catal. A:Gen. 103, 1993, 223–232.

[16] D. Sheldon, “Methanol Production – A Technical History,” Johnson Matthey Technol. Rev. 61, (3), 2017, 172–182.

[17] M. Kulawska and M. Madej-Lachowska, “Copper/zinc catalysts in hydrogenation of carbon oxides,” Chem. Process Eng. - Inz. Chem. i Proces. 34, (4), 2013, 479–496.

[18] M. Pérez-Fortes, J. C. Schöneberger, A. Boulamanti, and E. Tzimas, “Methanol synthesis using captured CO_2 as raw material: Techno-economic and environmental assessment,” Appl. Energy. 161, 2016, 718–732.

[19] M. Behrens, “Coprecipitation: An excellent tool for the synthesis of supported metal catalysts – From the understanding of the well known recipes to new materials,” Catal. Today. 246, 2015, 46–54.

[20] S. Kühl, A. Tarasov, S. Zander, I. Kasatkin, and M. Behrens, “Cu-based catalyst resulting from a Cu,Zn,Al hydrotalcite-like compound: A microstructural, thermoanalytical, and in situ XAS study,” Chem. - A Eur. J. 20, (13), 2014, 3782–3792.

[21] S. A. Kondrat, P. J. Smith,L. Luc, J.K. Bartley, S.H. Taylor, M. S. Spencer, G. J. Kelly, C. W. Park, C. J. Kiely, and G.J. Hutchings , “Preparation of a highly active ternary Cu-Zn-Al oxide methanol synthesis catalyst by supercritical CO_2 anti-solvent precipitation,” Catal. Today. 317, (1), 2018, 12-20.

[22] H. Ren, C.-H. Xu, H.-Y. Zhao, Y.-X. Wang, J. Liu, and J.-Y. Liu, “Methanol synthesis from CO_2 hydrogenation over Cu/γ-Al_2O_3 catalysts modified by ZnO, ZrO_2 and MgO,” J. Ind. Eng. Chem. 28, 2015, 261–267, Aug. 2015.

[23] E. L. Kunkes, F. Studt, F. Abild-Pedersen, R. Schlögl, and M. Behrens, "Hydrogenation of CO_2 to methanol and CO on $Cu/ZnO/Al_2O_3$: Is there a common intermediate or not?," J. Catal. 328, 2015, 43–48.

[24] C. Baltes, S. Vukojevic, and F. Schuth, "Correlations between synthesis, precursor, and catalyst structure and activity of a large set of $CuO/ZnO/Al_2O_3$ catalysts for methanol synthesis," J. Catal. 258, (2), 2008, 334–344.

[25] P. Villa, P. Forzattl, G. Buzzl-Ferrarls, G. Garone, and I. Pasquon, "Synthesis of Alcohols from Carbon Oxides and Hydrogen. 1. Kinetics of the Low-Pressure Methanol Synthesis," Ind. Eng. Chem. Process Des. Dev. 24, (1), 1985, 12–19.

[26] J. C. J. Bart and R. P. A. Sneeden, "Copper-zinc oxide-alumina methanol catalysts revisited," Catal. Today. 2, (1), 1987, 1–124.

[27] K. M. Vanden Bussche and G. F. Froment, "A Steady-State Kinetic Model for Methanol Synthesis and the Water Gas Shift Reaction on a Commercial $Cu/ZnO/Al_2O_3$ Catalyst," J. Catal. 161, (1), 1996, 1–10.

[28] G. C. Chinchen, P. J. Denny, D. G. Parker, M. S. Spencer, and D. A. Whan, "Mechanism of methanol synthesis from $CO_2/CO/H_2$ mixtures over copper/zinc oxide/alumina catalysts: use of ^{14}C-labelled reactants," Appl. Catal. 30, 2, 1987, 333–338.

[29] G. H. Graaf, E. J. Stamhuis, and A. A. C. M. Beenackers, "Kinetics of low-pressure methanol synthesis," Chem. Eng. Sci. 43, (12), 1988, 3185–3195.

[30] K. Kobl, S. Thomas, Y. Zimmermann, K. Parkhomenko, and A. C. Roger, "Power-law kinetics of methanol synthesis from carbon dioxide and hydrogen on copper-zinc oxide catalysts with alumina or zirconia supports," Catal. Today. 270, 2016, 31–42.

[31] X. Wang, H. Zhang, and W. Li, "In situ IR studies on the mechanism of methanol synthesis from CO/H_2 and CO_2/H_2 over $Cu\text{-}ZnO\text{-}Al_2O_3$ catalyst," Korean J. Chem. Eng. 27, (4), 2010, 1093–1098.

[32] F. Arena, K. Barbera, G. Italiano, G. Bonura, L. Spadaro, and F. Frusteri, "Synthesis, characterization and activity pattern of $Cu–ZnO/ZrO_2$ catalysts in the hydrogenation of carbon dioxide to methanol," J. Catal., vol. 249, (2), 2007, 185–194.

[33] F. Arena, G. Italiano, K. Barbera, G. Bonura, L. Spadaro, and F. Frusteri, "Basic evidences for methanol-synthesis catalyst design," Catal. Today, 143, (1–2), 2009, 80–85.

[34] Y. Choi, K. Futagami, T. Fujitani, and J. Nakamura, "Role of ZnO in Cu/ZnO methanol synthesis catalysts - morphology effect or active site model?," Appl. Catal. A Gen. 208, (1–2), 2001, 163–167.

[35] M. Behrens, F. Studt, I. Kasatkin, S. Kühl, M. Hävecker, F. Abild-pedersen, S. Zander, F. Girgsdies, P. Kurr, B. L. Kniep, M. Tovar, R. W. Fischer, J. K. Nørskov, R. Schlögl , "Industrial Catalysts," Science. 759, 80, 2012, 893–898.

[36] T. Fujitani and J. Nakamura, "The chemical modification seen in the Cu/ZnO methanol synthesis catalysts," Appl. Catal A: Gen. 191, 2000, 111–129.

[37] Y. Matsumura and H. Ishibe, "Effect of zirconium oxide added to Cu/ZnO catalyst for steam reforming of methanol to hydrogen," J. Mol. Catal. A Chem. 345, (1–2), 2011, 44–53.

[38] Z. Xu, Z. Qian, L. Mao, K. Tanabe, and H. Hattori, "Methanol synthesis from CO_2 and H_2 over CuO-ZnO catalysts combined with metal oxides under 13 atm pressure," Bulletin of Chemical Society Japan, 64, 1991, 1658–1663.

[39] G. Bonura, M. Cordaro, C. Cannilla, F. Arena, and F. Frusteri, "The changing nature of the active site of Cu-Zn-Zr catalysts for the CO_2 hydrogenation reaction to methanol," Appl. Catal. B Environ. 152–153, 2014, 152–161.

[40] K. Li and J. G. Chen, "CO_2 Hydrogenation to Methanol over ZrO_2-Containing Catalysts: Insights into ZrO_2 Induced Synergy," ACS Catal. 9, (9), 2019, 7840–7861.

[41] R. A. Koeppel and A. Baiker, "Copper/zirconia catalysts for the synthesis of methanol from carbon dioxide Influence of preparation variables on structural and catalytic properties of catalysts," 84, 1992, 77–102.

[42] Y. Wang, S. Kattel, W. Gao, K. Li, P. Liu, J.G. Chen, and H. Wang, "Exploring the ternary interactions in $Cu–ZnO–ZrO_2$ catalysts for efficient CO_2 hydrogenation to methanol," Nat. Commun., 10, (1), 2019.

[43] S. Kattel, B. Yan, J. G. Chen, and P. Liu, "CO_2 hydrogenation on Pt, Pt/SiO_2 and Pt/TiO_2: Importance of synergy between Pt and oxide support," J. Catal. 343, 2016, 115–126.

[44] L. I. Fan and T. Oc, "Development of Active and stable supported noble metal catalysts for hydrogenation of carbon dioxide to Methanol a," 36, (6), 1995, 633–636.

[45] Y. Hartadi, D. Widmann, and R. J. Behm, "Methanol synthesis: Via CO_2 hydrogenation over a Au/ZnO catalyst: An isotope labelling study on the role of CO in the reaction process," Phys. Chem. Chem. Phys. 18, (16), 2016, 10781–10791.

[46] H. Sakurai and M. Haruta, "Synergism in methanol synthesis from carbon dioxide over gold catalysts supported on metal oxides," 29, 1996, 361–365.

[47] S. Sugawa, K. Sayama, K. Okabe, and H. Arakawa, "Methanol synthesis from CO_2 and H_2 over silver catalyst," Energy Convers. Manag. 36, (6–9), 1995, 665–668.

[48] Y. Zhang, L. Zhong, H. Wang, P. Gao, X. Li, S. Xiao, G. Ding, W. Wei, and Y. Sun , "Catalytic performance of spray-dried $Cu/ZnO/Al_2O_3/ZrO_2$ catalysts for slurry methanol synthesis from CO_2 hydrogenation," J. CO_2 Util. 15, 2016, 72–82.

[49] M. Bukhtiyarova, T. Lunkenbein, K. Kähler, and R. Schlögl, "Methanol Synthesis from Industrial CO_2 Sources: A Contribution to Chemical Energy Conversion," Catal. Letters. 147, (2), 2017, 416–427.

[50] Y. Wang, W. Wang, Y. Chen, J. Ma, and R. Li, "Synthesis of dimethyl ether from syngas over core-shell structure catalyst $CuO-ZnO-Al_2O_3@SiO_2-Al_2O_3$," Chem. Eng. J. 250, 2014, 248–256.

[51] L. Li, D. Mao, J. Yu, and X. Guo, "Highly selective hydrogenation of CO_2 to methanol over CuO–ZnO–ZrO_2 catalysts prepared by a surfactant-assisted co-precipitation method," J. Power Sources. 279, 2015, 394–404.

[52] K. Samson, M. Sliwa, R.P. Socha, K. Gora-Marek, D. Mucha, D. Rutkowska-Zbik, J.F. Paul, M. Ruggiero-Mikolajczyk, P. Grabowsk, and J. Sloczynski, "Influence of ZrO_2 structure and copper electronic state on activity of Cu/ZrO_2 catalysts in methanol synthesis from CO_2," ACS Catal. 4, (10), 2014, 3730–3741.

[53] P. Gao, R. Xie, H. Wang, L. Zhong, L. Xia, A. Zhang, W. Wei, and Y. Sun, "Cu/Zn/Al/Zr catalysts via phase-pure hydrotalcite-like compounds for methanol synthesis from carbon dioxide," J. CO_2 Util. 11, 2015 41–48.

[54] A. Le Valant, C. Comminges, C. Tisseraud, C. Canaff, L. Pinard, and Y. Pouilloux, "The Cu-ZnO synergy in methanol synthesis from CO_2, Part 1: Origin of active site explained by experimental studies and a sphere contact quantification model on Cu + ZnO mechanical mixtures," J. Catal. 324, 2015 41–49.

[55] L. Angelo, K. Kobl, L. M. M. Tejada, Y. Zimmermann, K. Parkhomenko, and A.-C. Roger, "Study of $CuZnMO_x$ oxides (M=Al, Zr, Ce, CeZr) for the catalytic hydrogenation of CO_2 into methanol," Comptes Rendus Chim. 18, (3), 2015, 250–260.

[56] H. Jeong, C. H. Cho, and T. H. Kim, "Effect of Zr and pH in the preparation of Cu/ZnO catalysts for the methanol synthesis by CO_2 hydrogenation," React. Kinet. Mech. Catal. 106, (2), 2012, 435–443.

[57] M. S. Shaharun, A. Naeem, P. Ahmad, I. U. Din, and S. Tasleem, "Revalorization of CO_2 for methanol production via ZnO promoted carbon nanofibers based $Cu-ZrO_2$ catalytic hydrogenation," J. Energy Chem. 39, 2019, 68-76.

[58] X. An, J. Li, Y. Zuo, Q. Zhang, D. Wang, and J. Wang, "A Cu/Zn/Al/Zr fibrous catalyst that is an improved CO_2 hydrogenation to methanol catalyst," Catal. Letters. 118, (3–4), 2007, 264–269.

[59] M. Sánchez-Contador, A. Ateka, P. Rodriguez-Vega, J. Bilbao, and A. T. Aguayo, "Optimization of the Zr Content in the $CuO-ZnO-ZrO_2$/SAPO-11 Catalyst for the Selective Hydrogenation of $CO+CO_2$ Mixtures in the Direct Synthesis of Dimethyl Ether," Ind. Eng. Chem. Res. 57, (4), 2018, 1169–1178.

[60] J.F. Portha, K. Parkhomenko, K. Kobl, A.C. Roger, S. Arab, J.M. Commenge, and L. Falk, "Kinetics of Methanol Synthesis from Carbon Dioxide Hydrogenation over Copper-Zinc Oxide Catalysts," Ind. Eng. Chem. Res. 56, (45), 2017, 13133–13145.

[61] M. Behrens, D. Brennecke, F. Girgsdies, S. Kißner, A.Trunschke, N. Nasrudin, S. Zakaria, N. Idris, S. Hamid, B. Kniep, R. Fischer, W. Busser, M. Muhler, and R. Schlögl, "Understanding the complexity of a catalyst synthesis: Co-precipitation of mixed Cu,Zn,Al hydroxycarbonate precursors for $Cu/ZnO/Al_2O_3$

catalysts investigated by titration experiments," Appl. Catal. A Gen. 392, (1–2), 2011, 93–102.

[62] J.W. Evans, M.S. Wainwright, A.J. Bridgewater, and D.J. Young, " On the determination of copper surface area by reaction with nitrous oxide", Appl. Catal. 7, 1983, 75-83.

[63] G.C. Chinchen, C.M. Hay, H.D. Vandervell, and K.C. Waugh, " The measurement of copper surface areas by reactive frontal chromatography", J. Catal. 86, 1987, 79-86.

[64] K. Kobl, PhD Thesis of the University of Strabourg, "Aspects mécanistiques et cinétiques de la production catalytique de méthanol à partir de CO_2/H_2", https://www.theses.fr/2015STRAF023, 2015.

[65] J. W. Evans, M. S. Wainwright, and D. J. Young, "OXIDE," 7, 1983, 75–83.

[66] L. Angelo, M. Girleanu, O. Ersen, C. Serra, K. Parkhomenko, and A.-C. Roger, "Catalyst synthesis by continuous coprecipitation under micro-fluidic conditions: Application to the preparation of catalysts for methanol synthesis from CO_2/H_2", Catal. Today. 270, 2015, 59–67.

[67] X. Liu, P. Ramírez de la Piscina, J. Toyir, and N. Homs, "CO_2 reduction over Cu-ZnGaMO (M = Al, Zr) catalysts prepared by a sol-gel method: Unique performance for the RWGS reaction," Catal. Today. 296, 2017, 181–186.

[68] X. Liu, J. Toyir, P. Ramírez de la Piscina, and N. Homs, "Hydrogen production from methanol steam reforming over Al_2O_3 and ZrO_2 modified $CuOZnOGa_2O_3$ catalysts," Int. J. Hydrogen Energy. 42, (19), 2017, 13704–13711.

[69] F. Arena, R. Giovenco, T. Torre, A. Venuto, and A. Parmaliana, "Activity and resistance to leaching of Cu-based catalysts in the wet oxidation of phenol," Appl. Catal. B Environ. 45, (1), 2003, 51–62.

[70] G. Bonura, F. Arena, G. Mezzatesta, C. Cannilla, L. Spadaro, and F. Frusteri, "Role of the ceria promoter and carrier on the functionality of Cu-based catalysts in the CO_2-to-methanol hydrogenation reaction," Catal. Today. 171, (1), 2011, 251–256.

[71] M. C. Biesinger, L. W. M. Lau, A. R. Gerson, and R. S. C. Smart, "Resolving surface chemical states in XPS analysis of first row transition metals, oxides and hydroxides: Sc, Ti, V, Cu and Zn," Appl. Surf. Sci. 257, (3), 2010, 887–898.

[72] M. B. Fichtl, J. Schumann, I. Kasatkin, N. Jacobsen, M. Behrens, R. Schlögl, M. Muhler, and O. Hinrichsen, "Counting of oxygen defects versus metal surface sites in methanol synthesis catalysts by different probe molecules," Angew. Chemie - Int. Ed. 53, (27), 2014, 7043–7047.

[73] F. Arena, G. Mezzatesta, G. Zafarana, G. Trunfio, F. Frusteri, and L. Spadaro, "How oxide carriers control the catalytic functionality of the Cu-ZnO system in the hydrogenation of CO_2 to methanol," Catal. Today. 210, 2013, 39–46.

Graphical abstract